INL/CON-17-41598
PREPRINT

A High Performance Low Temperature Direct Carbon Fuel Cell

15th International Symposium on Solid Oxide Fuel Cells (SOFC-XV)

Wei Wu, Dong Ding, Maohong Fan, Ting He

April 2017

A High Performance Low Temperature Direct Carbon Fuel Cell

Wei Wu[a], Dong Ding* [a], Maohong Fan[b], Ting He[a]

[a] Idaho National Laboratory, Idaho Falls, ID 83415
[b] School of Energy Sources, University of Wyoming, Laramie, WY82071

A high performance direct carbon fuel cell is developed, where Ni-$Gd_{0.1}Ce_{0.9}O_{2-x}$ cermet, a molten carbonate composite, and $Sm_{0.5}Sr_{0.5}CoO_3$ are used as anode, electrolyte, and cathode, respectively. The cell can be operated at relatively low temperatures with power densities of 188, 108 and 48 $mWcm^{-2}$ being achieved at 600, 550, and 500^oC, respectively, when graphite-carbonate and CO_2-O_2 mixture are used as fuel and oxidant.

Introduction

Fuel cells are promising power generation techniques, having high energy conversion efficiency and low emissions (1, 2). Direct carbon fuel cells (DCFCs) operate on the same electrochemical principle as conventional fuel cells but using solid carbon as fuel, resulting in close to 100% fuel utilization and CO_2 capture ready (3). Therefore, the DCFC technology promises direct and efficient utilization of abundant solid carbon reserves in the world (4). When operated at elevated temperatures (>300^oC), the DCFC technology can be broadly classified into two main groups upon the types of electrolyte used:

1. Molten salt electrolyte: molten carbonate electrolyte (DC-MCFC) (5-7) and molten hydroxide electrolyte (DC-MHFC) (8-10).
2. Solid Electrolyte: defined as a solid oxide fuel cell (SOFC) directly using solid carbon as fuel (DC-SOFC) (11-13).

The molten salt electrolyte based DCFCs can reduce the resistance of anode owing to facilitated oxidation of the carbon in molten carbonates. However, this type of DCFCs has some disadvantages, including complex CO_2 management, sluggish oxygen reduction reaction (ORR) at the cathode and severe corrosion of cell components in molten carbonates (14). Therefore, the solid electrolyte based designs are comparatively robust as the anode and cathode are physically separated and no corrosion issue is involved. As a result, yttria stabilized zirconia (YSZ) and doped ceria, which have been extensively studied in solid oxide fuel cell (SOFC), were adopted as solid electrolytes for DCFCs. Excellent results have been reported for YSZ (15) and samarium doped ceria (SDC) (16) based DCFCs at temperatures higher than 700^oC. Limited results are available so far at reduced temperatures, due largely to the insufficient ionic conductivities of these electrolytes (17). However, high operating temperature leads to reverse Boudouard reaction and decreases the energy conversion efficiency (14). More importantly, problems associated with the high temperature operation, such as fast degradation, sealing issues, utilization of expensive materials, slow response to rapid start-up, and poor thermal cycling are hardly to overcome. To reduce the operating temperature of DC-SOFCs, two promising approaches have been conducted: developing highly conductive electrolyte and applying novel cathode material with high ORR ability at lower temperatures (18-20). Thus, development of fast ionic conductor and highly active cathode materials is imperative. Solid composite electrolytes composed of molten hydroxides or carbonates and oxygen ion conducting porous solid phases have been used in SOFCs at reduced temperatures (19, 21-

24). The conductivity of this kind of composite electrolyte, which composed of an O^{2-} conductive porous phase such as GDC and a CO_3^{2-}conductive molten carbonate phase, is much higher than that of the conventional solid electrolytes, YSZ and doped ceria in temperatures above 470◦C (25). Also, $Sm_{0.5}Sr_{0.5}CoO_3$ (SSC) material has been shown superior electro-catalytic activity and excellent stability at temperatures below 600°C (26-28). By applying SDC embedded $Sm_{0.5}Sr_{0.5}CoO_{3-\delta}$ (SSC) composite fibers as cathode, a maximum power density of 360 $mWcm^{-2}$ was achieved at 550°C (26). Electrochemical properties of CO_2-treated SSC/Co_3O_4 cathode triggered applications of in single-chamber fuel cells with direct hydrocarbon fuels operating at temperatures below 500°C (27). A relatively low firing temperature of SSC, compared to the conventional cathode materials such as $La_{0.8}Sr_{0.2}MnO_{3-\delta}$, and $La_{0.6}Sr_{0.4}Co_{0.2}Fe_{0.8}O_{3-\delta}$, could benefit the application of molten carbonate composite electrolyte (29).

Evidence manifested that direct electrochemical oxidation of carbon could occur at lower temperature (<700 °C) in DC-SOFC system when gadolinium doped ceria (GDC) was used as the electrolyte (30). This implied feasibility of DCFC operated at reduced temperatures. When DC-SOFC operates at reduced temperatures (e.g. <700°C), unlike hydrogen/hydrocarbons-fueled SOFC, one of the key challenges is that the reactant cannot readily reach the reaction region, typically triple-phase-boundary (TPB), thus the performance is restricted. The design of the anode as well as the fuel composition is thus of great importance for high-performing DC-SOFCs. Recent developed hybrid direct carbon fuel cell (HDCFC) technology, by dispersing solid carbon particulates in a molten carbonate to extended anode active, has been demonstrated improved performance in a solid-electrolyte system (31-34). When adding silver based catalysts (Ag, Ag_2O, Ag_2CO_3) into the carbon-carbonate slurry, the HDCFC performance could be further improved (35).

In this study, we applied a highly conductive GDC-carbonate composite electrolyte, highly active SSC cathode and hybrid fuel composition (commercially available graphite with carbonate) in the cell configuration and demonstrated excellent performances at temperatures below 600°C. The electrochemical tests were performed in Ar as the purge gas and 70%CO_2-30%O_2 as the oxidant. The reaction mechanism was also discussed.

Experimental

Fabrication of Electrolyte Supported Button Cells

Fabrication of composite carbonate-GDC electrolyte was reported previously (36). First of all, lithium–potassium carbonate, $Li_{0.67}K_{0.33}CO_3$, was formed by high-energy ball milling (SPEX SamplePrep LLC, NJ, USA) of Li_2CO_3 and K_2CO_3 in a mole ratio of 2:1 for 20 mins, followed by calcination at 600°C for 2 h. Secondly, composite electrolyte powder was obtained through mixing GDC powders and carbonate in a weight ratio of 3:7 and subsequent calcination at 700°C for 1 h. After quenching, the composite powders were uniaxially pressed at 300 Mpa and fired at 750°C for 4 hrs to form electrolyte pellets with a diameter of 10 mm. The SSC powders were synthesized using a glycine-nitrate process (37). The cathode (70wt% SSC and 30wt% GDC) and anode (60wt% NiO and 40% GDC) were screen printed on the each side of electrolyte pellet followed by co-sintering at 750°C for 2h. The active area is 0.178 cm^{-2}.

Composite Electrolyte Conductivity Measurement

The total conductivity was measured in air in the temperatures range from 400–650°C with electrochemical impedances spectroscopy (EIS) using Solartron 1400 Cell Test System. The composite electrolyte pellet was prepared by uniaxial pressing the premixed powders under a pressure of 280 MPa. Silver paste (Ag paste 9547, ESL ElectroScience Inc. USA) was printed on both sides of pellet and fired at 700^{o}C for 1 h as current collectors. The measurements were carried out in the frequency range from 0.1 Hz to 1 MHz with a bias voltage of 10 mV.

Cell Testing and Characterization

Button cells were sealed on an alumina tube using Aremco 552 sealant, with the anode side up. Silver mesh was used as current collectors with attached silver wires as leads. A 0.2 g mixture of fuel particles was filled into the anode chamber. Two types of carbon fuels were used in this research, with the weight ratio of carbon to Li_2CO_3–K_2CO_3 being 4:1. Ceramic cotton was stuffed in the tube near the carbon fuel to prevent the solid carbon from flowing away while reducing and purging with gas. Hydrogen was used during ramping. After NiO was fully reduced to metallic Ni, Ar gas with a flow rate of 10 ml min^{-1} was swept in as purge gas. Oxygen and carbon dioxide (volume ratio of 30:70) with total rate 40 ml min^{-1} was fed as cathode gas. A schematic illustration of the cell configuration is shown in Figure 1. I-V and I-P measurements, as well as electrochemical impedance spectroscopy (EIS) were recorded using a Solartron 1400 electrochemical working station when a stable open circuit voltage (OCV) was observed. The cell cross-section before and after tests were imaged via JEOL 6700F, equipped with back scattering electron (BSE) analyzer. The structure of the electrolyte was analyzed with a Rigaku SmartLab X-Ray Diffraction (XRD) in 15-90^{o} angular range with 0.04 step size and a 1.6s resonance time.

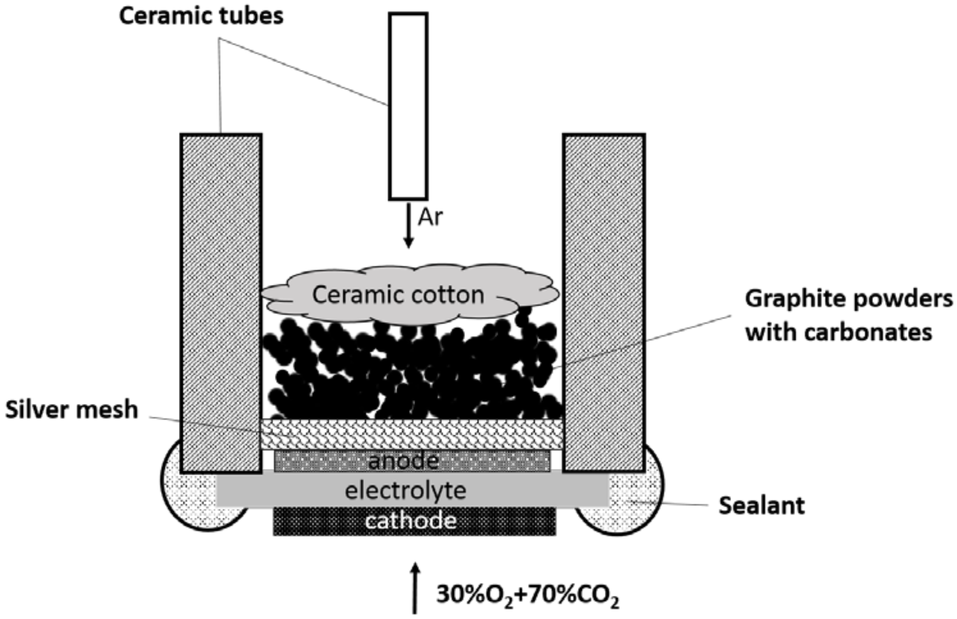

Figure 1. The schematic illustration of DCFC testing set up in this research.

Results and Discussion

Electrochemical Properties of GDC-carbonate Composites

Figure 2 shows the Arrhenius plot of the total conductivities of GDC-carbonate composite, GDC, and YSZ electrolytes as a function of temperature. The composite was sintered at 750°C for 4h, while the GDC and YSZ were sintered at 1400°C. According to the figure, a sharp drop in the plot for carbonate composite occurred at approximately 475 °C, which was close to the melting point of Li_2CO_3–K_2CO_3 carbonate, 490 °C. When the temperature was 500°C, the total conductivity of composite electrolyte is 0.047 S cm^{-1}, indicating a factor of 15 and 235 times higher than GDC and YSZ, respectively. Our previous results suggested that the conductivity of the GDC-carbonate electrolyte highly depend on the volume fraction, especially at lower temperatures (36). Figure 3 shows the cross-sectional image of a GDC-carbonate composite electrolyte based DCFC cell after testing. The distribution of both GDC and carbonate phases was uniform and continuous. No cracks were observed both at the cathode/electrolyte and anode/electrolyte interfaces. Although the GDC phase was not dense and the electrolyte seemed porous, no leak of gases through the electrolyte happened due to the fact that the pores and cracks in GDC phase were filled and wetted with molten carbonate (18). That was confirmed in OCV observation in our electrochemical testing.

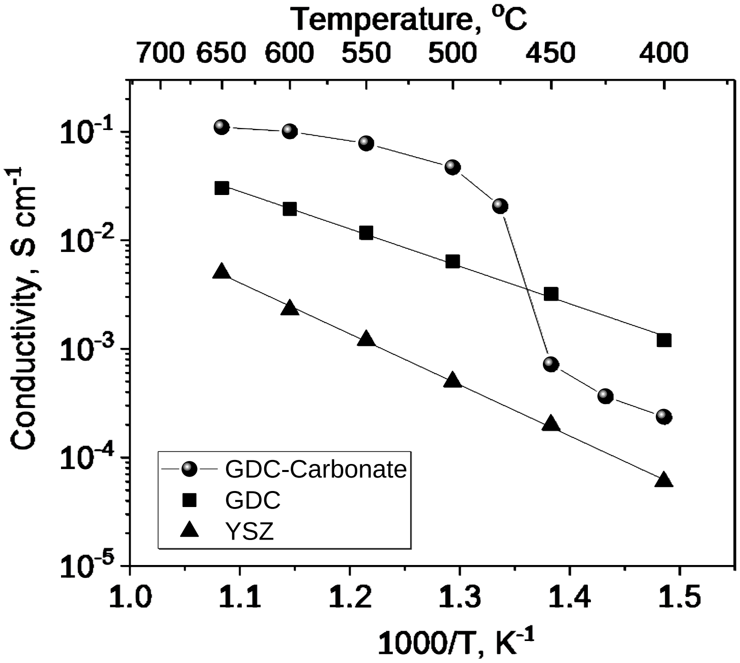

Figure 2. Temperature dependence of the conductivity measured in air for GDC-carbonate, GDC and YSZ.

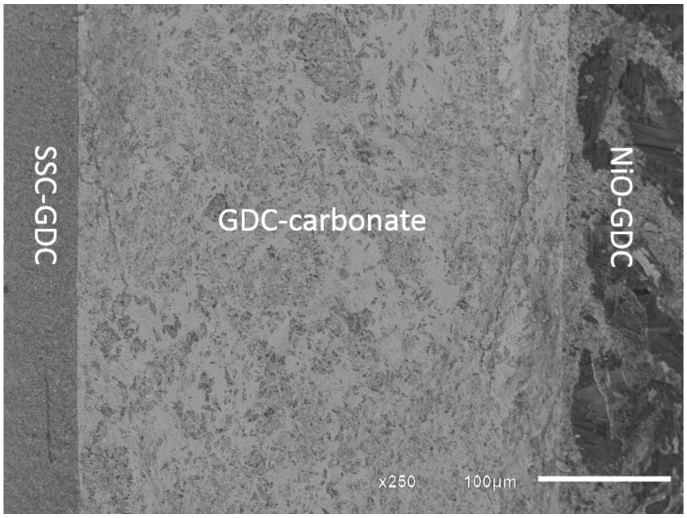

Figure 3. Cross-sectional image of composite electrolyte based cell after testing

Electrochemical Performance of GDC-carbonate composite electrolyte supported DCFCs

Figure 4 shows current–voltage (IV) characteristics and the corresponding power densities of a DCFC at temperatures 500-600°C. Theoretically, the OCV of a DCFC with oxygen as oxidant is independent to temperature because carbon is always in its elementary state (4), which is in good accordance with what were observed in this research. As shown in Figure 4, the OCVs stay at approximately 1.08V at temperature range of 500-600^{o}C. The OCVs were close to the theoretical values, indicating there was no gas crossover. The maximum power density of the cell presented the similar trend against temperature. The maximum power densities (MPD) reached 188 mWcm^{-2} and 108 mWcm^{-2} at 600 ^{o}C and 550 ^{o}C, respectively. When the temperature further decreased to 500 ^{o}C, which is close to the melting point of Li_2CO_3–K_2CO_3 carbonate, a maximum power density of 48 mWcm^{-2} was obtained. This value was even comparative to the performance of GDC based DCFC at 700^{o}C, which was reported to be 50 mWcm^{-2} (30). Moreover, the cell performance is superior to an electrolyte-supported HDCFC with a peak power density of 113.1Wcm^{-2} at 650^{o}C reported by Xu. et al. (14), which was the best performance at such a low temperature ever reported. The good performance at low temperature may attribute to both the high conductivity of the composite electrolyte and superior ORR activity of SSC (27). Our results suggested the feasibility of directly electrochemical oxidation of solid carbon in a DCFC at 500-600^{o}C, and there is a large space in performance improvement, given that the anode configuration, cathode microstructure and fuel composition can be further optimized.

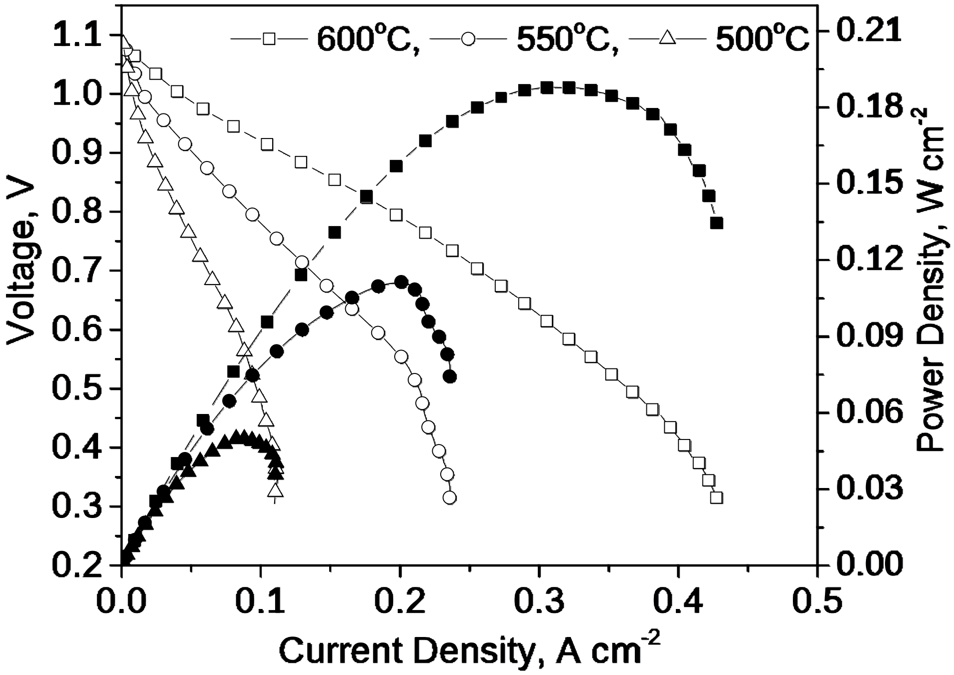

In the present cell configuration, both CO_3^{2-} and O^{2-} ions are transporting species when CO_2/O_2 mixture is applied to the cathode. The oxygen molecules are directly reduced into oxygen ions and also react with CO_2 to generate carbonate ions. In anode side, carbon is oxidized by CO_3^{2-} and O^{2-} ions forming CO_2. The anode and cathode reactions can be expressed as:

Cathode side reaction:

$$O_2 + 4e^- \rightarrow 2O^{2-} \quad [2]$$

$$O_2 + 2CO_2 + 4e^- \rightarrow 2CO_3^{2-} \quad [3]$$

Anode side reaction:

$$C + 2O^{2-} \rightarrow CO^2 + 4e^- \quad [4]$$

$$C + 2CO_3^{2-} \rightarrow 3CO_2 + 4e^- \quad [5]$$

Conclusions

A high performance DCFC has been demonstrated by applying GDC-Li/Na_2CO_3 composite as electrolyte, SSC as cathode and hybrid solid carbon as the fuel. The electrochemical performance were tested at temperatures from 500 to 600°C. The OCV reached 1.08 V at 600°C, indicating a good sealing and no gas leakage across the composite electrolyte. When using graphite-carbonates mixed powders as fuel, the cell presented promising performance at temperatures below 600°C. A maximum power density of 48 mWcm^{-2} was obtained at 500°C with O_2 and CO_2 as the oxidant. The significant improvement of the catalytic activity at low temperature attributes to both the synergistic conduction of CO_3^{2-} and O^{2-} in the composite electrolyte and the superior ORR activity of SSC cathode. Our approach suggested a great prospective of developing high performance DCFCs at reduced temperature.

Acknowledgements

The authors gratefully acknowledge the Idaho National Laboratory Directed Research and Development Program under DOE Idaho Operations Office Contract DE-AC07-05ID14517 for the support of this work.

Reference

1. D. Ding, X. X. Li, S. Y. Lai, K. Gerdes and M. L. Liu, *Energy Environ Sci*, **7**, 552 (2014).
2. W. Wu, W. B. Guan, G. L. Wang, F. Wang and W. G. Wang, *Advanced Energy Materials*, **4** (2014).
3. W. W. Jacques, Method of converting potential energy of carbon into electrical energy, in, Google Patents (1896).
4. S. Giddey, S. P. S. Badwal, A. Kulkarni and C. Munnings, *Progress in Energy and Combustion Science*, **38**, 360 (2012).
5. I. Rexed, C. Lagergren and G. Lindbergh, *International Journal of Hydrogen Energy*, **39**, 12242 (2014).
6. Y. Hishinuma and T. Abe, *International Conf on Coal, the Environment and Development : Technologies to Reduce Greenhouse Gas Emissions*, 447 (1992).
7. L. Plomp, J. B. J. Veldhuis, E. F. Sitters and S. B. Vandermolen, *Journal of Power Sources*, **39**, 369 (1992).
8. E. M. Patton, S. Zecevic and P. Parharni, *Proceedings of the 4th International Conference on Fuel Cell Science, Engineering, and Technology, Pts A and B*, 463 (2006).
9. J. Yang, H. Muroyama, T. Matsui and K. Eguchi, *Journal of Power Sources*, **245**, 277 (2014).
10. L. Guo, J. M. Calo, E. DiCocco and E. J. Bain, *Energy & Fuels*, **27**, 1712 (2013).
11. K. Hemmes, J. F. Cooper and J. R. Selman, *International Journal of Hydrogen Energy*, **38**, 8503 (2013).
12. Y. Nabae, K. D. Pointon and J. T. S. Irvine, *Energy Environ Sci*, **1**, 148 (2008).
13. F. Yu, Y. Zhang, L. Yu, W. Cai, L. Yuan, J. Liu and M. Liu, *International Journal of Hydrogen Energy*, **41**, 9048 (2016).
14. X. Xu, W. Zhou, F. Liang and Z. Zhu, *International Journal of Hydrogen Energy*, **38**, 5367 (2013).
15. Y. H. Bai, Y. Liu, Y. B. Tang, Y. M. Xie and J. Liu, *International Journal of Hydrogen Energy*, **36**, 9189 (2011).
16. B. B. Yang, R. Ran, Y. J. Zhong, C. Su, M. O. Tade and Z. P. Shao, *Angewandte Chemie-International Edition*, **54**, 3722 (2015).
17. S. P. S. Badwal and K. Foger, *Ceram Int*, **22**, 257 (1996).
18. L. Jia, Y. Tian, Q. Liu, C. Xia, J. Yu, Z. Wang, Y. Zhao and Y. Li, *Journal of Power Sources*, **195**, 5581 (2010).
19. W. Li, C. Y. Xiong, L. C. Jia, J. Pu, B. Chi, X. Chen, J. W. Schwank and J. Li, *Journal of Power Sources*, **284**, 272 (2015).
20. H. V. P. Nguyen, M. G. Kang, H. C. Ham, S. H. Choi, J. Han, S. W. Nam, S. A. Hong and S. P. Yoon, *Journal of the Electrochemical Society*, **161**, F1458 (2014).
21. L. Fan, C. Wang, J. Di, M. Chen, J. Zheng and B. Zhu, *J Nanosci Nanotechno*, **12**, 4941 (2012).
22. N. Jaiswal, S. Upadhyay, D. Kumar and O. Parkash, *Ceram Int*, **41**, 15162 (2015).

23. R. Raza, H. Y. Qin, L. D. Fan, K. Takeda, M. Mizuhata and B. Zhu, *Journal of Power Sources*, **201**, 121 (2012).
24. L. D. Fan, C. Y. Wang, M. M. Chen, J. Di, J. M. Zheng and B. Zhu, *International Journal of Hydrogen Energy*, **36**, 9987 (2011).
25. B. Zhu, *Journal of Power Sources*, **114**, 1 (2003).
26. J. Choi, B. Kim and D. Shin, *Journal of the European Ceramic Society*, **33**, 2269 (2013).
27. H. Z. Zhang, H. Y. Liu, Y. Cong and W. S. Yang, *J Power Sources*, **185**, 129 (2008).
28. D. Ding, Z. B. Liu, L. Li and C. R. Xia, *Electrochem Commun*, **10**, 1295 (2008).
29. D. Ding, B. B. Liu, Z. Zhu, S. Zhou and C. R. Xia, *Solid State Ionics*, **179**, 896 (2008).
30. A. Kulkarni, S. Giddey and S. P. S. Badwal, *Solid State Ionics*, **194**, 46 (2011).
31. X. Xu, W. Zhou, F. Liang and Z. Zhu, *Applied Energy*, **108**, 402 (2013).
32. L. Deleebeeck and K. K. Hansen, *Journal of Solid State Electrochemistry*, **18**, 861 (2014).
33. J. Ruflin, A. D. Perwich, C. Brett, J. K. Berner and S. M. Lux, *Journal of Power Sources*, **213**, 275 (2012).
34. C. R. Jiang, J. J. Ma, A. D. Bonaccorso and J. T. S. Irvine, *Energy & Environmental Science*, **5**, 6973 (2012).
35. L. Deleebeeck, D. Ippolito and K. K. Hansen, *Electrochimica Acta*, **152**, 222 (2015).
36. W. Zhu, C. Xia, D. Ding, X. Shi and G. Meng, *Materials Research Bulletin*, **41**, 2057 (2006).
37. C. R. Xia, W. Rauch, F. L. Chen and M. L. Liu, *Solid State Ionics*, **149**, 11 (2002).